Multi-Objective Optimization for Bidirectional Electric Vehicle Charging Stations

Bara, I.; Mouli, G. R. Chandra; Bauer, P.

DOI
10.1109/OAJPE.2025.3614816

Publication date
2025

Document Version
Final published version

Published in
IEEE Open Access Journal of Power and Energy

Citation (APA)
Bara, I., Mouli, G. R. C., & Bauer, P. (2025). Multi-Objective Optimization for Bidirectional Electric Vehicle Charging Stations. *IEEE Open Access Journal of Power and Energy*, *12*, 652-663.
https://doi.org/10.1109/OAJPE.2025.3614816

Received 3 March 2025; revised 10 June 2025 and 20 August 2025; accepted 22 September 2025.
Date of publication 26 September 2025; date of current version 2 October 2025.

Digital Object Identifier 10.1109/OAJPE.2025.3614816

Multi-Objective Optimization for Bidirectional Electric Vehicle Charging Stations

ISTVÁN BARA (Student Member, IEEE),
GAUTHAM RAM CHANDRA MOULI (Member, IEEE),
AND PAVOL BAUER (Senior Member, IEEE)

Department of Electrical Sustainable Energy, Delft University of Technology, 2628 CD Delft, The Netherlands
CORRESPONDING AUTHOR: G. R. CHANDRA MOULI (G.R.ChandraMouli@tudelft.nl)

This work was supported by European Union's Horizon Europe Research and Innovation Program through the project Flexible Energy Systems Leveraging the Optimal Integration of EVs Deployment Wave (FLOW) under Grant 101056730.

ABSTRACT The increasing number of electric vehicles (EVs) means both a challenge and an opportunity for the electric grid. Different charging algorithms have been proposed in the literature to tackle these specific challenges and make use of the potential services that EVs can provide. However, to properly investigate the conflicting objectives, a multi-objective approach is paramount. These algorithms provide a family of solutions instead of just one, so the decision-maker can see the connection and trade-offs between the objectives. This paper proposes a highly customisable multi-objective framework based on an expanded version of the augmented ε-constraint 2 method. Together with a mixed integer linear programming (MILP) formulation, it is used to solve a charging station scheduling problem. An energy management system (EMS) executes the calculated schedules to show the effect on the individual EVs. Numerical simulations based on market and EV data from the Netherlands demonstrate the adaptability and effectiveness of the proposed algorithm.

INDEX TERMS Charging station, electric vehicle, energy management system, multi-objective optimization, smart charging, V2G.

I. INTRODUCTION

Over the past few years, concerns about climate change and its effects have gained more and more traction. One possible way of reducing greenhouse gasses, especially CO_2 emissions, is the electrification of the transport sector [1]. The sales of Electric Vehicles (EVs) have risen continuously in the last decade. More than 10 million EVs were sold globally in 2022, and another 35% growth was projected for 2023.

The increasing number of EVs will significantly impact the power grid because of the substantially increased electricity demand for charging the vehicles [2]. On the other hand, with proper charging strategies and using vehicle-to-grid (V2G) technology, EVs can also offer services to the grid, increasing grid stability and helping the energy transition [3]. Examples include frequency regulation, peak shaving and load levelling. These services can also provide financial benefits to multiple actors of the electricity system, including EV users [4], [5]. At the same time, their objectives often contradict each other, creating trade-offs. Based on the objectives and investigated scenarios, different optimisation approaches and methods were investigated in the literature [6], [7], but these mainly focus on one specific objective. This approach does not make it possible to fully utilise the possibilities provided by EVs.

With multi-objective (MO) optimisation, the relationship between the objectives becomes clear. This way, the most suitable solution can be selected for each situation. This paper introduces a multi-objective optimisation algorithm suitable for EV charging stations. It focuses on the local level (i.e. a single charging station), but it will form the basis for future work exploring the cooperation possibilities between stations and grid-level control. Thus, it is of paramount importance that the algorithm can be customised and easily modified or expanded.

A. LITERATURE REVIEW

Smart and bidirectional charging algorithms can range from small-scale home energy management systems [8], [9] to parking lots with up to a couple hundred EVs [5], [10], [11]

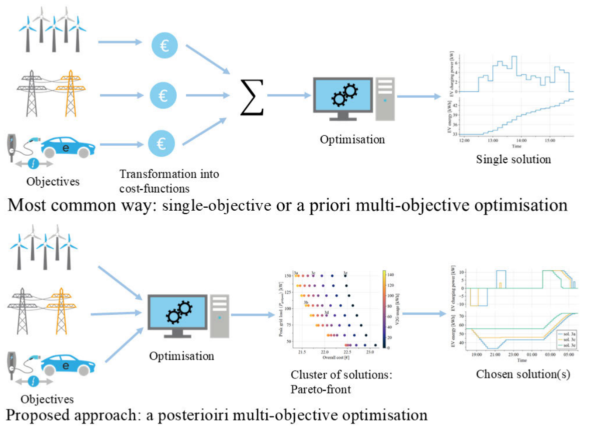

FIGURE 1. Schematic representation of the cost-based optimisation (top) and a posterioiri optimisation (bottom).

to large aggregates of up to 10 000 vehicles [12], [13]. Most papers focus on specific aspects of the scheduling problem, for example, the uncertainties regarding the availability of the EVs [4], [11] or the forecast for photovoltaic systems connected to the chargers [5], [8]. Another important aspect is the control architecture, which includes centralised [14] and decentralised approaches [12], as well as hierarchical systems [15]. Researchers also considered different timescales with fixed timestep [16], multi-level [9] and event-driven algorithms [17]. Different charging station, EV and battery degradation models have been researched, as well. However, the overwhelming majority of papers only include one objective, which is the minimisation of cost. Even though a cost function could include multiple aspects, this is a limiting factor. Some objectives might hinder others, and the trade-off is hard to identify with only cost-based formulation. Moreover, only one actor's (EV user, Transmission System Operator (TSO), Distribution System Operator (DSO), etc.) perspective is usually considered. A multi-objective formulation is necessary to overcome these limitations. A schematic representation of the two approaches is shown in fig. 1.

In the case of multi-objective optimisation, two or more conflicting objectives are defined. There are multiple possible classifications for these problems. One of the most popular ones is based on the decision-making process [18], [19]:

- A priori methods where preference information is available before the solution process.
- A posteriori methods where first possible (Pareto-optimal) solutions are identified, and the decision-making process chooses one of the solutions.
- Progressive methods where the generated solutions are iteratively refined based on the decision-maker's preferences.

Both a prioiri and a posterioiri methods have been investigated in the literature for EV charging scheduling. In the former case, the multi-objective problem is always transformed into one or more single-objective formulations. The weighted sum method [17], [20], [21] and hierarchical optimisation [22], [23], [24] are two commonly used approaches, but these only provide one Pareto-optimal solution and do not represent the whole front. In the former case, multiple solutions can be generated by changing the weights and re-running the oprimisation. A posterioiri methods include mathematical programming, metaheuristic algorithms and machine learning. Their common point is that they generate multiple nondominated solutions, which represent part of or the whole Pareto-front. With mathematical programming, different scalarisations are formed and then solved using single-objective optimisation. Metaheuristic algorithms approximate the front in a single run, which consists of multiple iterations.

The number of papers dealing with EV scheduling based on a posteriori methods is relatively small, but metaheuristic approaches seem more prevalent [25], [26], [27]. Unfortunately, with these methods, the optimality cannot be guaranteed [28]. Furthermore, they do not provide control over the distribution of the found solutions. Among the scalarisation methods, the augmented ε-constraint method is the most often used [29], [30]. These papers demonstrate the potential of the mathematical programming approach, but they lack customisability, as the number and order of objectives are fixed. table 1 summarizes the main differences between the mentioned multi-objective approaches and highlights the advantages of the algorithm proposed in this paper.

B. CONTRIBUTIONS

The main contributions of the work reported below include:

- The paper introduces a highly-customisable multi-objective optimisation algorithm for EV charging scheduling based on the augmented ε-constraint 2 (AUGMECON2) [33] method. Most optimisation settings can be easily accessed and changed by the user, including the number and order of objectives, the grid density for each objective and the overall search area. The algorithm is also independent of the underlying problem formulation and solver. These allow the user to fully utilise the multi-objective optimisation approach in different scenarios.
- The AUGMECON2 method has been modified to increase the flexibility of the algorithm. These changes influence the implementation and also add a new feature: secondary objectives. To the authors' knowledge, this feature has not been proposed before.
- A Mixed-Integer Linear Programming (MILP) formulation is presented for a charging station scheduling problem. The four main objectives represent the goals of different actors in the electricity system. Some of these objectives have been investigated in the literature, but not together. EVs not wishing to participate in smart charging or V2G are also accounted for. The formulation, in combination with the flexible MO algorithm, also allows for easy expansion possibilities.

TABLE 1. Comparison of the different multi-objective optimisation approaches.

Approach	References	Number of objectives	Number of secondary objectives	Optimality can be guaranteed	Control over the solutions space	Solver independent
Weighted sum	[17], [20], [21]	fixed	none	yes	very limited	yes
Hierarchical	[22]–[24]	fixed	none	yes	single solution	yes
Metaheuristic	[25]–[27], [31], [32]	fixed	none	no	limited	no
Augmented ε-constraint	[29], [30]	fixed	none	yes	limited	yes
Proposed algorithm	this paper	configurable	configurable	yes	full	yes

II. MULTI-OBJECTIVE FORMULATION

A. NOTATIONS

M	Number of primary objectives
O	Number of secondary objectives
$f_i(\mathbf{x})$	i^{th} objective
S_i	Surplus variable for the i^{th} objective
r_i	Range for the i^{th} objective
e_i	Calculated upper limit for the i^{th} objective
u_i	Upper bound for the i^{th} objective
it_i	Iteration counter for the i^{th} objective
int_i	Number of intervals for the i^{th} objective

B. DESCRIPTION OF THE ORIGINAL METHOD

For the multi-objective formulation, a mathematical programming approach, the augmented ϵ-constraint was chosen. The implementation is based on an improved version of the method, AUGMECON2 [33]. The augmented ϵ-constraint method is based on scalarisation: the original multi-objective formulation is converted into multiple single-objective problems. With ϵ-constraint, one objective is optimised while the others are fixed to given values in a restricted range specified by the pay-off table. The ranges and chosen density determine the number of sub-problems that must be solved. The general problem formulation is as follows:

$$min f_1(\mathbf{x}) - \varepsilon \left(\frac{S_2}{r_2} + 10^{-1}\frac{S_3}{r_3} + \ldots + 10^{-(M-2)}\frac{S_M}{r_M} \right) \quad \text{(1a)}$$

$$\text{s.t.} \quad f_i(\mathbf{x}) + S_i = e_i \quad \forall i \in [2,\ M] \quad \text{(1b)}$$

$$e_i = u_i - \frac{r_i it_i}{int_i} \quad \forall i \in [2,\ M] \quad \text{(1c)}$$

The first step is the generation of the $M \times M$ pay-off table using the lexicographic method described in [34]. Each row is calculated by optimising the objectives in order and recording their value. However, after each step, the previously calculated optimal value is added as a constraint. The objective orders are varied, so each objective appears both in first and last place. The minimum and maximum value for each objective determines the range of possible objective values, r_i. The maximum value determines the original upper bound, u_i, which is then reduced at each iteration with a step size of $\frac{r_i}{int_i}$. The number of intervals in the given range, int_i is determined by the user. With more intervals, and thus grid points, a denser representation of the Pareto-front can be reached, but the computational power need also increases. The loops for the objectives are nested into each other so that the algorithm steps through each grid point. As the iteration counter increases, the given objective is constrained closer to its optimal value. It is also possible to manually define the upper bound, thus restricting the search space. A more detailed explanation, including the advantages of the AUGMECON2 method compared to the original method, is given in [33] and [34].

C. EXPANSIONS OF THE METHOD

1) NESTING STRUCTURE

Multiple objectives can be defined, but only the ones chosen by the user are passed to the solver. Thus, the number of objectives and their order can change. To step through all the grid points, M-1 nested loops are used in the original papers [33], [34], where M is fixed (hard-coded). To avoid this problem, a simulated nested loop structure was implemented, where a set of slots is maintained for each looping variable. This way, recursions are avoided, which could negatively impact the performance and memory usage. However, the number of objectives can still be changed only by setting the corresponding input (function argument); no code change is necessary.

2) HANDLING OF SITUATIONS WITH NO TRADE-OFF

As can be seen in eq. (1a), the surplus variables are scaled by the corresponding ranges. If there is no trade-off between two or more objectives, the corresponding ranges will be zero, and a division by zero error will occur. Some objectives might only conflict in certain situations, based on the electricity price, charging time, number of EVs, etc. To overcome this problem without changing the formulation, the algorithm was extended to detect these scenarios automatically. In these cases, the objectives are removed, and their optimal values are added as constraints, similar to the process in lexicographic optimisation. If only one objective remains, the algorithm switches to single-objective optimisation.

3) SECONDARY OBJECTIVES

Secondary objectives modify the calculated solutions without affecting the values of the primary objectives. Multiple different schedules might exist with the same primary objective value. For example, regarding the cost, such a situation can occur if the electricity price remains the same for a longer period. The charging can start earlier or later or could oscillate between on and off periods. With the proper secondary objective(s), the number of these schedules can be reduced to one, similar to Symmetry-breaking constraints. Otherwise, it can be hard to control which schedule is selected by the solver among several schedules with the same primary objective function value. Secondary objectives can also be used to evaluate specific objectives without affecting the main result (solutions on the Pareto-front).

The pay-off table described in section II-B must be extended to add secondary objectives. With O secondary objectives, the new table size will become $M \times (M + O)$. The secondary objectives are always put in the last places in the optimisation order when generating the table rows so as not to affect the primary objective values and ranges. For the same reason, their maximum (worst) value is selected and added as a constraint. These constraints are present for each grid point and are not modified in the iterations.

III. CHARGING STATION ENERGY MANAGEMENT SYSTEM

An energy management system (EMS) is necessary to control the charging of the EVs connected to the charging station. In this paper, the station is assumed to have solar panels and multiple chargers installed. The nominal solar power and the grid limits are configurable. The overall time window and the length of the timesteps can also be modified. Day-ahead optimisation with a rolling horizon is used in the case studies, as it can showcase the capabilities of the proposed multi-objective framework.

IV. MATHEMATICAL FORMULATION OF THE SCHEDULING PROBLEM

The EV charging scheduling problem has been formulated as a mixed-integer linear program (MILP) for a public charging station. The variables, parameters, constraints and objectives are detailed in the following subsections.

A. INPUT VARIABLES AND PARAMETERS

t, j	Indeces for timestep and EV, respectively
$P^j_{\mathrm{EVmax+}}$	Maximum charging power of the j^{th} EV [kW]
$P^j_{\mathrm{EVmax-}}$	Maximum discharging power (V2G) of the j^{th} EV [kW]
E^j_{EVmax}	Maximum battery capacity of the j^{th} EV [kWh]
P^j_{PVmax}	Maximum (nominal) power of the connected PV panels [kW]
T	Length of the optimisation window (number of timesteps)
T_{step}	Length of one optimisation timestep in hours
$T^j_{\mathrm{arr}}, T^j_{\mathrm{dep}}$	Arrival and departure timestep of the j^{th} EV, respectively
$E^j_{\mathrm{EVs}}, E^j_{\mathrm{EVg}}$	Starting and target battery energy of the j^{th} EV, respectively [kWh]
η^j_{ch}	Converter efficiency of the j^{th} EV
$P^t_{\mathrm{gridmax+}}$	Maximum allowed grid load (feeding) at timestep t [kW]
$P^t_{\mathrm{gridmax-}}$	Maximum allowed grid load (drawing) at timestep t [kW]
$c^t_{\mathrm{buy}}, c^t_{\mathrm{sell}}$	Electricity buying and selling price (market clearing price) at timestep t, respectively [€/kWh]
c_{penalty}	Penalty paid to the EV user for not satisfying the charging need [€/kWh]
c_{PV}	Price for solar power (if applicable) [€/kWh]
SoC_{min}	Minimum SoC for each connected EV
α_{CVmin}	Ratio of the maximum charging power at 100% SoC and nominal maximum charging power
SoC_{high}	SoC threshold, above which the maximum charging power is reduced
SoC_{low}	SoC threshold, below which the maximum discharging power is reduced
N	Number of connected EVs
β_{FCR}	Fraction of a timestep for which the frequency regulation power must be maintained

B. OPTIMISATION VARIABLES

All variables are equal to or greater than zero.

$P^{t,j}_{\mathrm{EV+}}$	Charging power of the j^{th} EV at timestep t [kW]
$P^{t,j}_{\mathrm{EV-}}$	Discharging (V2G) power of the j^{th} EV at timestep t [kW]
$E^{t,j}_{\mathrm{EV}}$	Battery energy of the j^{th} EV at timestep t [kWh]
E^j_{unmet}	Unmet energy demand of the j^{th} EV (difference between the requested and actual battery energy at the time of departure) [kWh]
P^t_{PV}	Used solar power at timestep t [kW]
a^t_{grid}	Binary variable for grid power direction (0: power fed to the grid, 1: power drawn from the grid)
$P^t_{\mathrm{grid-}}$	Power fed to the grid at timestep t [kW]
$P^t_{\mathrm{grid+}}$	Power drawn from the grid at timestep t [kW]
P_{gridpeak}	Peak power drawn during the optimization window [kW]

$P^{t,j}_{\text{FCRu}}$	Maximum up-regulation power that can be offered as frequency regulation service [kW]
$P^{t,j}_{\text{FCRd}}$	Maximum down-regulation power that can be offered as frequency regulation service [kW]
$P^{t,j}_{\text{EVuc}}$	Charging power of the j^{th} uncontrolled EV at timestep t [kW]

C. ACCEPTANCE CRITERIA

The arriving EVs must meet the acceptance criteria. These ensure that a feasible charging schedule can be found. The maximum amount of energy that can be delivered to the given EV is limited by either the grid or the charger and EV. Equation (2a) represents the grid-based limit, eq. (2b) shows the same for the charger. P^t_{agg} is the aggregated charging schedule of all the already connected EVs. P^t_{avg} is the charging schedule of the EVs currently waiting to connect and is calculated based on their average power need. The stricter limit is then compared with the EV's energy need. If the requested energy exceeds the available capacity, the EV is rejected, and the user needs to modify the scheduled departure date or requested energy amount.

$$E^j_{\text{gridmax}} = \sum_{t=T^j_{\text{arr}}}^{T^j_{\text{dep}}} (P^t_{\text{gridmax}-} - P^t_{\text{agg}} - P^t_{\text{avg}}) T_{\text{step}} \eta^j_{\text{ch}} \quad \forall j \tag{2a}$$

$$E^j_{\text{chmax}} = (T^j_{\text{dep}} - T^j_{\text{arr}}) P^j_{\text{EVmax}+} T_{\text{step}} \eta^j_{\text{ch}} \quad \forall j \tag{2b}$$

$$min(E^j_{\text{gridmax}}, E^j_{\text{chmax}}) \geq E^j_{\text{EVg}} - E^j_{\text{EVs}} \quad \forall j \tag{2c}$$

D. CONSTRAINTS

1) EV CONSTRAINTS

Both the charging and discharging power ($P^{t,j}_{\text{EV}+}, P^{t,j}_{\text{EV}-}$) are limited by either the converter onboard the EV or the external charger. After the EV has connected to the charger, the limits can be compared, and the stricter limit is applied ($P^j_{\text{EVmax}+}, P^j_{\text{EVmax}-}$). The offered frequency regulation power ($P^{t,j}_{\text{FCRu}}, P^{t,j}_{\text{FCRd}}$) might further restrict the (dis)charging power. If an EV does not wish to participate in V2G operation, the maximum discharging power is set to zero. Please note, that either $P^{t,j}_{\text{EV}+}$ or $P^{t,j}_{\text{EV}-}$ is zero at all times.

$$P^{t,j}_{\text{EV}+} + (P^{t,j}_{\text{FCRd}} - P^{t,j}_{\text{EV}-}) \leq P^j_{\text{EVmax}+} \quad \forall t, \forall j \tag{3}$$

$$P^{t,j}_{\text{EV}-} + (P^{t,j}_{\text{FCRu}} - P^{t,j}_{\text{EV}+}) \leq P^j_{\text{EVmax}-} \quad \forall t, \forall j \tag{4}$$

The EV battery energy cannot exceed the maximum battery capacity.

$$E^{t,j}_{\text{EV}} \leq E^j_{\text{EVmax}} \quad \forall t, \forall j \tag{5}$$

The battery energy at the start of the optimisation is set based on the reported SoC and battery capacity of the EV.

$$E^{T^j_{\text{arr}},j}_{\text{EV}} = E^j_{\text{EVs}} \quad \forall j \tag{6}$$

At departure, the battery energy must be equal to the requested level from the EV user (E^j_{EVg}). The E^j_{unmet} term is added to avoid infeasible solutions. This is especially important with multi-objective optimisation towards the extreme points on the Pareto-front. The variable E^j_{unmet} cannot be negative. Thus, the overcharging of the battery is avoided.

$$E^{T^j_{\text{dep}},j}_{\text{EV}} + E^j_{\text{unmet}} = E^j_{\text{EVg}} \quad \forall j \tag{7}$$

Before arrival and after departure, the charging, discharging power, and offered regulation power are set to zero.

$$P^{t,j}_{\text{EV}+}, P^{t,j}_{\text{FCRd}} = 0 \quad \forall t \notin [T^j_{\text{a}}, T^j_{\text{dep}}], \forall j \tag{8}$$

$$P^{t,j}_{\text{EV}-}, P^{t,j}_{\text{FCRu}} = 0 \quad \forall t \notin [T^j_{\text{a}}, T^j_{\text{dep}}], \forall j \tag{9}$$

The battery energy level for each EV for each timestep is calculated with eq. (10). The charging and discharging efficiency are considered to be the same. The inclusion of this efficiency term also ensures that $P^{t,j}_{\text{EV}+}$ and $P^{t,j}_{\text{EV}-}$ are not both nonzero at the same time under normal market conditions. Thus, the addition of a binary variable is not necessary.

$$E^{t+1,j}_{\text{EV}} = E^{t,j}_{\text{EV}} + P^{t,j}_{\text{EV}+} T_{\text{step}} \eta^j_{\text{ch}} - P^{t,j}_{\text{EV}-} \frac{T_{\text{step}}}{\eta^j_{\text{ch}}}$$
$$\forall t \in [T^j_{\text{arr}}, T^j_{\text{dep}} - 1], \forall j \tag{10}$$

The EVs' maximum charging and discharging powers also depend on the SoC. The exact dependency is nonlinear, but a linear approximation is used in this work, so the problem can be formulated as a MILP. The maximum charging power is assumed to linearly reduce from the nominal value to $\alpha_{\text{CVmin}}\%$ of the nominal value if the EV is charged above the threshold SoC_{high}. Similarly, the maximum discharging power is reduced to zero below the threshold SoC_{low}.

$$P^{t,j}_{\text{EV}+} \leq -P^j_{\text{EVmax}+} \frac{1 - \alpha_{\text{CVmin}}}{1 - SoC_{\text{high}}} \left(\frac{E^{t,j}_{\text{EV}}}{E^j_{\text{EVmax}}} - 1 \right)$$
$$+ \alpha_{\text{CVmin}} P^j_{\text{EVmax}+} \quad \forall t, \forall j \tag{11}$$

$$P^{t,j}_{\text{EV}-} \leq \frac{P^j_{\text{EVmax}-}}{SoC_{\text{low}}} \frac{E^{t,j}_{\text{EV}}}{E^j_{\text{EVmax}}} \quad \forall t, \forall j \tag{12}$$

2) CHARGING STATION AND GRID CONNECTION CONSTRAINTS

The sum of incoming and outgoing power (from the charging station's point of view) at each timestep must be equal. $P^{t,j}_{\text{EVuc}}$ denotes the charging power of the uncontrolled EVs. These EVs do not participate in smart charging, their charging schedule is calculated before the optimisation algorithm is run. Two options are available, fast and average rate charging. In the former case, the EVs are charged at their maximum power until they reach the desired battery energy level. In the second case, the EVs are charged at a constant power (except above the SoC_{high} threshold) while connected.

$$\sum_{j=1}^{N} P^{t,j}_{\text{EV}+} + \sum_{j=1}^{N} P^{t,j}_{\text{EVuc}} + P^t_{\text{grid}-} =$$

$$= P^t_{\text{PV}} + P^t_{\text{grid}+} + \sum_{j=1}^{N} P^{t,j}_{\text{EV}-} \quad \forall t \tag{13}$$

The used solar power is limited by the maximum power of the panels. It is assumed that PV curtailment is possible.

$$P^t_{\text{PV}} \leq P^t_{\text{PVmax}} \quad \forall t \tag{14}$$

$P^t_{\text{grid}+}$ and $P^t_{\text{grid}-}$ cannot be nonzero at the same time. While with traditional cost-only based objectives, the difference between buying and selling price can ensure this condition, with multi-objective optimisation, the addition of a binary variable is necessary. Equations (15), and (16) also limit the drawn/fed power based on the maximum allowed grid load.

$$P^t_{\text{grid}+} \leq (1 - a^t_{\text{grid}}) P^t_{\text{gridmax}} \quad \forall t \tag{15}$$

$$P^t_{\text{grid}-} \leq a^t_{\text{grid}} P^t_{\text{gridmax}} \quad \forall t \tag{16}$$

E. OBJECTIVES

The objective formulations are recorded as expressions or variable-constraint combinations. Some constraints are only necessary for certain objectives; these are shown grouped together. Four possible primary objectives and one secondary objective are currently defined, but the list can easily be extended. The objectives and their formulations are as follows:

1) COST

The cost function is a multi-objective formulation in itself and it includes the price of electricity drawn from and fed to the grid ($c^t_{\text{buy}}, c^t_{\text{sell}}$), the price for the solar power (c^t_{PV}), and the penalty paid to the EV user for not satisfying the charging need (c_{penalty}). The first two terms have fixed coefficients which are based on the input data. The penalty term ensures that the EVs are always charged to the requested level if feasible. The solution space can be restricted to exclude the region where this penalty term becomes visible. Minimising E^j_{unmet} could also be a separate objective if, for example, fully charging the EVs is not required or if cost is not included in the used objectives. The cost term of obtaining PV energy is warranted if the panels are not owned by the charging station.

$$\begin{aligned} min \sum_{t=1}^{T} (c^t_{\text{buy}} P^t_{\text{grid}+} - c^t_{\text{sell}} P^t_{\text{grid}-}) T_{\text{step}} + \\ + \sum_{j=1}^{N} c_{\text{penalty}} E^j_{\text{unmet}} + \sum_{t=1}^{T} c^t_{\text{PV}} P^t_{\text{PV}} T_{\text{step}} \end{aligned} \tag{17}$$

2) PEAK GRID LOAD

There are two limits for the grid load in this formulation. P^t_{gridmax} represents a hard constraint that shall not be exceeded at any point. This could represent physical limits such as grid connection or transformer limits. P_{gridpeak} adds only a soft constraint that tries to limit the impact on the grid further. This objective can be used to follow a directive from the grid operator in times of grid congestion. Formulating it as an objective enables the identification of trade-offs as well.

$$P^t_{\text{grid}+} \leq P_{\text{gridpeak}} \quad \forall t \tag{18a}$$

$$P^t_{\text{grid}-} \leq P_{\text{gridpeak}} \quad \forall t \tag{18b}$$

$$min\, P_{\text{gridpeak}} \tag{18c}$$

3) DISCHARGED ENERGY (V2G USAGE)

V2G usage can increase the number of charging-discharging cycles an EV battery experiences, thus increasing the rate of battery degradation. eq. (19) tries to reduce this effect by minimising the discharged energy amount.

$$min \sum_{t=1}^{T} \sum_{j=1}^{N} P^{t,j}_{\text{EV}-} T_{\text{step}} \tag{19}$$

4) FREQUENCY REGULATION SERVICE

To provide frequency regulation service, part of the total available power and battery energy must be reserved. The available power and battery energy are calculated at the individual EV level. Equations (3) and (4) (introduced earlier) limit the offered power based on the available (dis)charging power, eqs. (20a) and (20b) restrict it based on the available battery energy. The latter constraints also set a minimum battery level while the EV is connected to the charger to avoid SoC levels that are too low. While overall, the regulation service is assumed to be energy neutral [35], the charging station must be able to maintain the regulation power for a certain amount of time. This length is determined by β_{FCR} relative to one timestep (T_{step}). The grid connection limits the available aggregated power; this is expressed in eqs. (20c) and (20d). The objective function (eq. (20e)) tries to maximise the average offered power. The regulation power ($P_{\text{FCRu}}, P_{\text{FCRd}}$) is set to zero, if the EV is not connected in the given timestep. If symmetrical bids are required, the formulation can be extended with eq. (20f).

$$\begin{aligned} E^{t,j}_{\text{EV}} \geq (P^{t,j}_{\text{FCRu}} - P^{t,j}_{\text{EV}+} + P^{t,j}_{\text{EV}-}) T_{\text{step}} \beta_{\text{FCR}} + \\ + SoC_{\text{min}} E^{t,j}_{\text{EVmax}} \quad \forall t,\ \forall j \end{aligned} \tag{20a}$$

$$\begin{aligned} E^{t,j}_{\text{EV}} \leq E^{t,j}_{\text{EVmax}} + \\ - (P^{t,j}_{\text{FCRd}} + P^{t,j}_{\text{EV}+} - P^{t,j}_{\text{EV}-}) T_{\text{step}} \beta_{\text{FCR}} \quad \forall t,\ \forall j \end{aligned} \tag{20b}$$

$$\sum_{j=1}^{N} (P^{t,j}_{\text{FCRu}} - P^{t,j}_{\text{EV}+} + P^{t,j}_{\text{EV}-}) \leq P^t_{\text{gridmax}-} \quad \forall t \tag{20c}$$

$$\sum_{j=1}^{N} (P^{t,j}_{\text{FCRd}} + P^{t,j}_{\text{EV}+} - P^{t,j}_{\text{EV}-}) \leq P^t_{\text{gridmax}+} - \sum_{j=1}^{N} P^{t,j}_{\text{EVuc}} \quad \forall t \tag{20d}$$

$$max \sum_{t=1}^{T} \sum_{j=1}^{N} \frac{P^{t,j}_{\text{FCRu}} + P^{t,j}_{\text{FCRd}}}{T} \tag{20e}$$

$$\sum_{j=1}^{N} P^{t,j}_{\text{FCRu}} = \sum_{j=1}^{N} P^{t,j}_{\text{FCRd}} \quad \forall t \tag{20f}$$

5) SECONDARY OBJECTIVE (FAST CHARGE)

A simple objective function, shown in eq. (21), was defined in the formulation to demonstrate the effect of secondary objectives. The objective is to keep the EVs' battery level as high as possible for most of the optimisation window. This ensures that the EVs are charged at the earliest opportunity (and discharged at the latest) and can be helpful if there is a high likelihood of unexpected (early) departure. Of course, this could negatively affect the batteries' health, because keeping the battery at high SoCs can increase calendar ageing [36].

$$max \sum_{t=1}^{T} \sum_{j=1}^{N} E_{\mathrm{EV}}^{t,j} \tag{21}$$

Any of the defined primary objectives can also be added as secondary objectives.

V. EVALUATION OF THE MO ALGORITHM

A. IMPLEMENTATION OF THE ALGORITHM AND USED DATASETS

The above-described algorithms were implemented in Julia, using the JuMP [37] modelling package. The package provides an intuitive modelling language and supports multiple solvers. The MILP formulation was solved by Gurobi in the following case studies.

The used datasets include solar data from a modeled reference 1 $\mathrm{kW_p}$ panel, day-ahead market (DAM) electricity prices and EV-related data. Both the solar and price data have a 1-minute resolution for one year. The details of the solar model can be found in [16]. The price data comes from the EPEX SPOT market and was acquired using the ENTSO-E platform [38]. The date chosen for both data sets was 02-01-2018. The EV dataset contains arrival and departure times, SoC (at arrival and departure) and battery information (maximum capacity and power). It was generated using distribution functions from Elaad [39] based on recorded charging sessions. The technical specifications were chosen to represent the 10 most common EVs in the Netherlands (source: RVO [40]). The power limits for charging and discharging are assumed to be symmetrical.

B. SIMULATION PARAMETERS

Unless otherwise stated, the following parameters were used for the scenarios. A public charging point was simulated, with 40 EVs arriving within 24 hours. It is assumed that only 70% of the EV users wish to participate in V2G, and 15% disallow smart charging as well. In the latter case, the EVs are charged at maximum power after arrival (fast uncontrolled charging). The number of EVs were chosen to represent a moderately-sized charging station. The 70% and 15% values create a more realistic scenario, where not all charging sessions are fully controllable. The optimisation window was extended by five hours to allow the last EVs to leave. The optimisation timestep (T_{step}) was 10 minutes. The selling price is assumed to be 90% of the buying price ($c_{\mathrm{sell}} = 0.9c_{\mathrm{buy}}$), $c_{\mathrm{PV}} = 0.01$€/kWh and the penalty term is

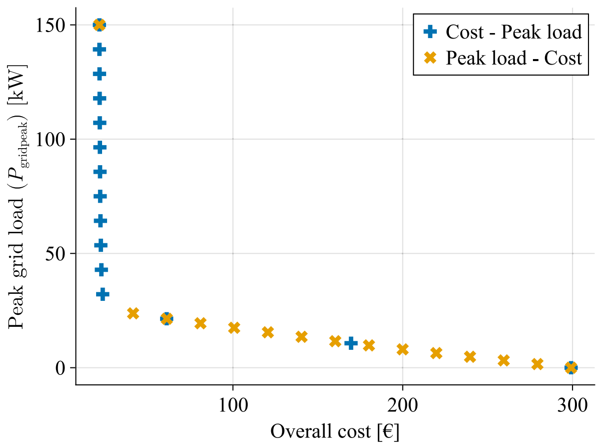

FIGURE 2. **Impact of the objective order on the Pareto-front.**

$c_{\mathrm{penalty}} = 0.5$€/kWh. This is a relatively low value (10× the maximum DAM price), but its effect is clearly visible in the cost values. The grid power limit (P_{gridmax}) was set to 150 kW for each timestep in both directions. Regarding the EV batteries, $SoC_{\mathrm{min}} = 0.2$, $SoC_{\mathrm{high}} = 0.85$, $SoC_{\mathrm{low}} = 0.1$, $\beta_{\mathrm{FCR}} = 1$ and α_{CVmin} was set to 0.2. The EMS was operating in day-ahead mode.

C. GENERATED SCENARIOS

This section aims to showcase the versatility and capabilities of the proposed algorithm and prove the importance of the a posteriori mathematical optimisation approach.

1) DISTRIBUTION OF SOLUTIONS

There are an infinite number of theoretical solutions on the Pareto-front, but optimisation algorithms can only generate a finite number of solution points. The distribution of these points has a huge effect on how representative the generated front is. A proper distribution also helps the decision-maker correctly identify the trade-offs and choose the most suitable solution. The proposed algorithm provides three methods to influence the distribution of the generated points.

- Changing the number of intervals (int_i)
- Changing the objective order
- Restricting the search-space

The number of intervals influences the density of the generated solutions for the given objective. More important objectives could have a denser representation, but a high number of intervals can affect the performance significantly, resulting in longer computational times.

The proposed method first estimates the feasible ranges for all objectives. Then, it creates a number of sub-problems by dividing the second and further objectives into multiple intervals. These intervals are then enforced by adding constraints for the maximum values of the objectives. As a result, the found solutions on the Pareto-front will be mostly evenly distributed along the 2nd, 3rd, etc., dimensions (axes), but

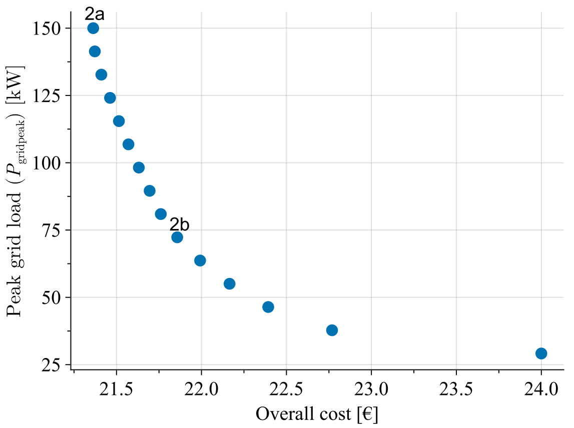

FIGURE 3. **Pareto-front with two objectives and restricted search-space.**

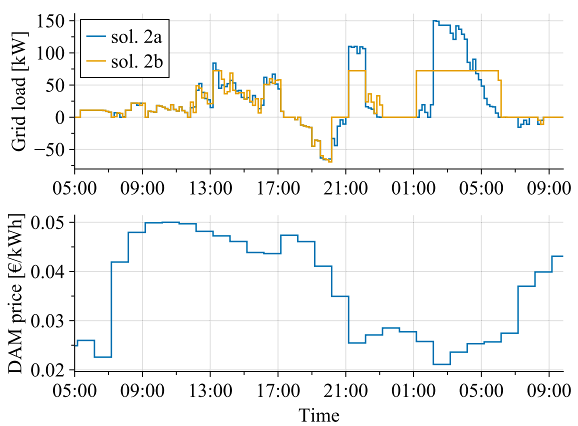

FIGURE 4. **Pareto-front with two objectives and restricted search-space.**

the same cannot be said for the first objective. By varying the objective order, evenly distributed solutions among the (previously) first objective's dimension can be found as well. Fig. 2 demonstrates the impact of the objective order. There is an overlap between the two sets of solutions, because they belong to the same Pareto-front.

Restricting the search-space helps to generate more solutions in the most important areas, without increasing the number of intervals. The restriction can be achieved by modifying the calculated feasible ranges of the objectives. Then the algorithm automatically adds the necessary constraints during the generation of the sub-problems. In fig. 3, the cost value was set to be below 24 €, focusing on the high-gradient area of the Pareto-front.

2) IDENTIFICATION OF TRADE-OFFS WITH TWO OBJECTIVES

In this scenario, only two objectives were selected: cost minimisation (eq. (17)) and peak grid load reduction (eq. (18c)) in this order. The resulting Pareto-front, depicted in fig. 3, shows

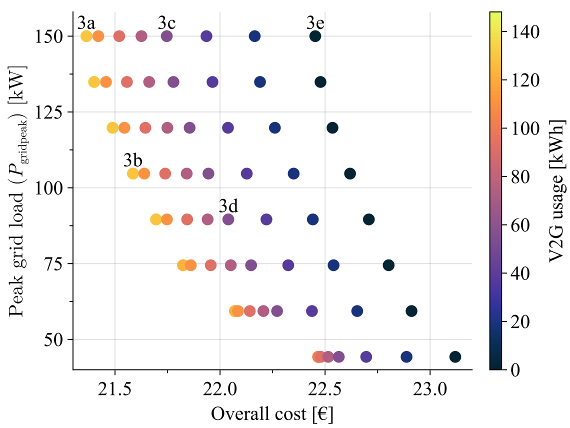

FIGURE 5. **Pareto-front with three objectives.**

the trade-off between the two objectives. Please note that the solution-space was restricted in this case, as described in the previous section. Higher costs indicate that some EVs were not charged according to their demand, so these solutions are disregarded. The sudden increase in costs is due to the penalty term in eq. (17). The steep first section in the figure shows that the trade-off is minimal in this region. Compared to solution 2a (lowest cost), solution 2b offers more than 50% reduction in grid load (from 150 kW to 72 kW) while only increasing the costs by around 2.4% (from 21.36 € to 21.87€). Thus, the charging station could accept significantly more EVs without the risk of considerably increasing the relative costs. The reason for the increasing costs is shown in fig. 4. With solution 2b the station is forced to charge at higher electricity prices.

3) IDENTIFICATION OF TRADE-OFFS WITH THREE OBJECTIVES

In this scenario, the objective to reduce the discharged energy (V2G) (eq. (19)) was also added as the third objective. The objective value ranges of objectives 2 and 3 were divided into eight intervals. The search space was restricted to cost values below 24 € to maintain scale. Fig. 5 shows the calculated representation of the Pareto-front. From the figure, it is clear that the values of peak grid load and V2G usage can be drastically changed with minimal cost change. This shows the advantage of the family of solutions offered by multi-objective optimisation. With single-objective optimisation, only certain, usually extreme solutions could be found, with no way of identifying the trade-offs.

Five solutions were chosen to show the effect of the multi-objective optimisation on the scheduling, shown in fig. 5. Solutions 3a and 3e represent two extreme solutions for objectives 1: lowest cost and 3: lowest discharged energy, respectively. There is only one extreme point for cost, as that is the main objective, but there are multiple points with zero V2G usage. Solution 3b aims to reduce the peak grid load, but it also slightly lowers the V2G usage. Solution 3c signif-

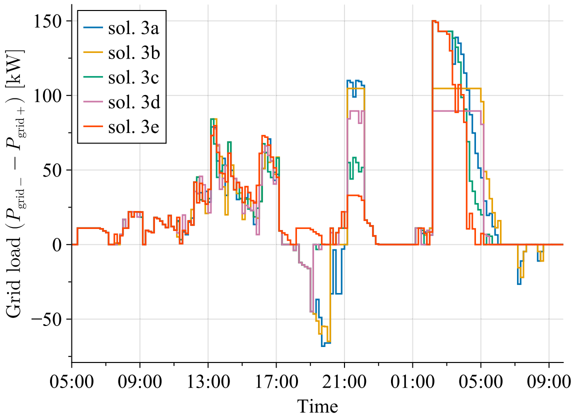

FIGURE 6. Grid load profiles of the chosen solutions (fig. reffig:2dcolor).

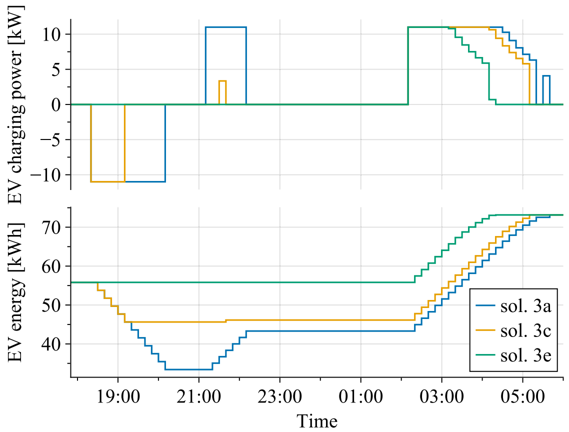

FIGURE 7. Charging power and battery energy profiles of the chosen solutions (fig. reffig:2dcolor) for one EV.

icantly reduces the V2G usage while leaving the peak grid load unaffected. Solution 3d reduces both objective values, with some increase in cost compared to solution 3c.

Figure. 6 shows the grid load throughout the day with different solutions. The peak grid load reduction effect can be seen in the evening around 21:00 and after midnight around 02:00, where the load curve is flattened and the maximum value is lower. The reduction in V2G is mostly visible in the afternoon around 18:00. The effect of objective 3 is clearly visible on EV-level as well, which is shown in fig. 7. As expected, solution 3c reduces the amount of discharged energy, and solution 3e does not allow any.

The three objectives can represent different actors and their goals. The charging station operator wants to reduce the charging costs, the EV owner wants to avoid battery degradation, and the grid operator needs to avoid congestion.

4) IDENTIFICATION OF TRADE-OFFS WITH FOUR OBJECTIVES

Frequency regulation service provision (eq. (20e)) was added as the fourth objective in this scenario. Equation (20f) was

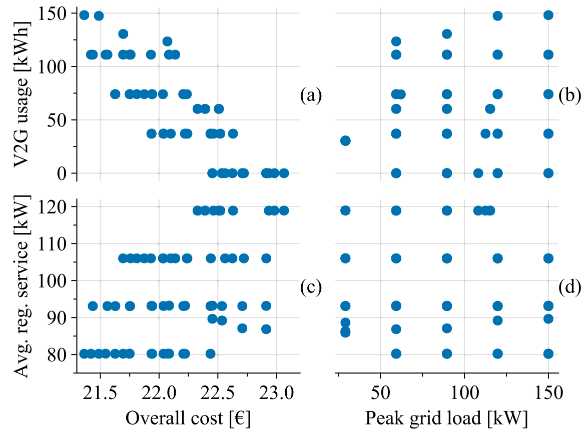

FIGURE 8. Partial SPLOM of the Pareto-front with 4 objectives.

added to force symmetrical up- and downregulation power values. The number of intervals for each objective was reduced to 4, which still results in a maximum of 125 solutions. One way to visualise a four-dimensional Pareto-front is to use a ScatterPLOt Matrix (SPLOM), where the relationship of any two objectives can be investigated.

For clarity, only a part of the whole SPLOM is shown in fig. 8. Subplot (a) shows a clear trade-off between the charging cost and the V2G usage. Lowering the discharged energy amount always results in a higher cost, but at the same time, choosing a higher-cost solution also guarantees that the V2G usage can be lowered regardless of the other objectives. This can be seen by the lack of solution in the upper right corner of the plot.

A similar relationship can be found between the offered regulation power and the charging cost (subplot (c)), but in this case, a higher cost does not always guarantee higher available regulation power. The minimum regulation power only starts increasing after the 22.5; cost value.

The two right subplots ((b) and (d)) show a more even distribution of solutions. This means more possible combinations of objective values, the objectives do not restrict each other. Of course, there is still a trade-off, but it manifests in the remaining objective(s). The decision-maker could infer even more information with colour-coding or numbering of the solutions to see the cross-effects. However, static plots offer limited assistance as the number of objectives increases. Interactive tools or automated decision-making algorithms are necessary to effectively deal with higher-dimension objective spaces.

5) SECONDARY OBJECTIVE

Fig. 9 illustrates the effect of the secondary objective (eq. (21)) on the grid load and an individual EV's charging schedule. The base case was solution 3a. The objective values remain unaffected, thus the grid load only shows minor changes. The change is more noticeable on the EV-level: instead of two on-off cycles at around 3:30 and 4:00, the

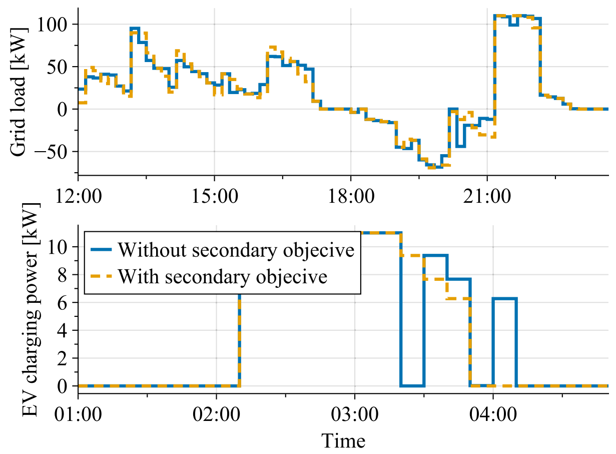

FIGURE 9. **Effect of the secondary objective on the grid load (top) and an individual EV (bottom).**

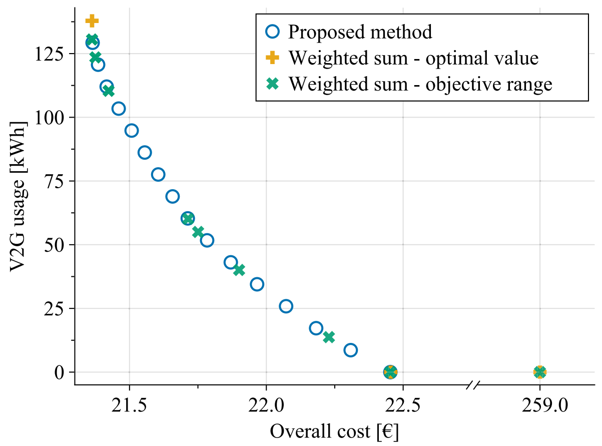

FIGURE 10. **Comparison of the proposed method and the weighted sum method.**

TABLE 2. **Benchmark results.**

Objectives	No. of intervals and sub-problems	Time (median) [s]	Time (mean $\pm \sigma$) [s]
1-2	14 (15)	14.88	14.94 $\pm$ 0.38
1-2	28 (29)	26.91	26.94 $\pm$ 0.52
1-3	14 (15)	8.67	8.65 $\pm$ 0.35
1-3	28 (29)	14.20	14.21 $\pm$ 0.50
1-4	14 (15)	18.30	18.40 $\pm$ 0.43
1-2-3	8×8 (81)	45.49	45.44 $\pm$ 0.27
1-2-3-4	4×4×4 (125)	130.00	129.90 $\pm$ 0.95

TABLE 3. **Benchmark results for the weighted sum method.**

Objectives	No. of intervals and sub-problems	Time (median) [s]	Time (mean $\pm \sigma$) [s]
1-2	14 (15)	9.98	10.05 $\pm$ 0.27
1-2	28 (29)	17.92	17.85 $\pm$ 0.81
1-3	14 (15)	4.87	4.95 $\pm$ 0.34
1-2-3	11 (78)	22.77	23.05 $\pm$ 1.1

solver chooses to charge continuously and then stop. Other similar modifications could be achieved with the appropriate secondary objective.

6) BENCHMARKS

Benchmarks were run to assess the performance of the algorithm with different objectives and numbers of intervals. The results are summarised in table 2. The numbers denote the objectives in the same order as they were introduced: eqs. (17), (18c), (19) and (20e). The computation times are given for the whole algorithm. This includes loading the input data, generating the pay-off table, solving the sub-problems and evaluating the solutions using the EMS. The benchmarks were run on a laptop with an Intel i7-1265U CPU and 16 GB of RAM. The results are based on 20 samples for each combination of objectives and interval numbers.

Both the number of intervals and the type of objective have a strong effect on the computation time. The number of intervals directly influences the number of sub-problems to be solved. Therefore, focusing on the right area of the objective space is paramount. The type of objective changes the complexity of the sub-problems, because some enforce more constraint than others, as described in section IV-E.

While the objectives are fixed for a certain situation, the number of intervals can be changed to balance the computational power need. The solving times could also be further reduced by using parallel computation, as the sub-problems are independent of each other. However, as can be seen from the results, even with a high-number of sub-problems the solve time is well below the timestep value of 10 minutes. Thus, the problem could be scaled up to include more EVs, or a longer timeframe.

D. COMPARISON WITH DIFFERENT METHODS

1) WEIGHTED SUM METHOD

In the weighted sum method, the objectives ($f_i(\mathbf{x})$) are multiplied with different weights (w_i) and then added together to generate a single aggregated objective, as shown in eq. (22).

$$min \sum_{i=1}^{N} w_i f_i(\mathbf{x})/f_i^{norm} \tag{22}$$

The sub-problems are generated by modifying the weights in a way that their sum is always equal to 1. The objectives are also usually normalised to avoid bias due to their different scales. Two different normalising factors (f_i^{norm}) were investigated in this study. Using the optimal value of the respective objective function, as suggested in [30], and using the calculated objective ranges, which are also used in the proposed algorithm.

In fig. 10 a 2 objective example can be seen. The number of sub-problems was the same for all three cases. The choice of the normalising factor has a huge effect on the results. Using the objective ranges improves the distribution of solutions significantly, but the proposed method still provides better results. The weighted sum method also gives dominated solutions towards the extreme points.

The summary of the computational performance can be seen in table 3. The same settings were used as in the original benchmarks. The weighted sum method has a clear advantage in terms of solve time over the AUGMECON2 approach, especially as the number of sub-problems increases. If speed is the main priority, and an accurate representation of the Pareto-front is less important, then the weighted sum method with carefully chosen normalising factors could be a viable alternative.

2) METAHEURISTIC METHODS

Unlike with the weighted sum method, a direct comparison with metaheuristic methods was not possible because the JuMP modelling package does not support derivative-free solving methods. For the direct comparison, a new model would have to be built using a different modelling language. Here, metrics defined in [25] and [41] are given for the proposed method, and examples from the literature are used for further comparison.

The distance from the optimal solution(s) can be measured using accuracy and generational distance, while precision refers to the repeatability. The proposed formulation is mostly linear; it only has a limited number of binaries, which can also be omitted in certain cases. Thus, the output of the solver is deterministic, and the optimality of the solutions can be guaranteed. It also means that all of these metrics are always zero, the method provides equal, or better results, than metaheuristic methods. Numerical examples can be found in [25], where the authors use the Satisfiability Modulo Theory to find the optimal solutions and use them as a reference for their proposed heuristic method. In [31] the authors claim that their method outperforms the non-heuristic method, but they use a linear approximation for the comparison. References [26], [27] and [32] do not provide similar metrics.

Evenness (ξ) and distribution metrics (DM) are used to quantify the diversity of solutions on the Pareto-front. These metrics are only reported in [25]; the rest mainly focus on a single selected solution. As explained in the previous sections, the extended AUGMECON2 method provides fine control over both the solution space and the distribution of solutions. This is reflected in the low values of these metrics, which were calculated for the first three cases in the benchmarks section (table 2) with a search space limited to below 23€ overall cost. These are: $\xi = 0.7532, 0.7685, 0.3901$ and $\mathrm{DM} = 0.0724, 0.0378, 0.0435$, respectively.

Total solve time is where metaheuristic algorithms show an advantage, especially in the case of large-scale or non-linear formulations. References [25] and [31] present numerical comparisons. It is important to note that the computational power of the computers used in the different studies varies significantly.

VI. CONCLUSION

In this paper, a highly customisable multi-objective framework has been proposed together with a MILP formulation of a charging station scheduling problem. The importance of the multi-objective approach has been demonstrated using case studies. It has been shown how the resulting Pareto-front can be used to investigate the trade-offs and their effects on the resulting schedules.

The additional information that this approach provides can be invaluable to both Charging Point Operators (CPOs) and Policy Makers. For CPOs it can not only help fine-tune the daily operations, but can also help prepare for future scenarios, such as higher EV-penetration and stricter grid limits. Policy Makers can use the results to propose realistic monetary incentives for objectives that support the grid but do not provide a direct benefit to the participants in the electricity market.

REFERENCES

[1] International Energy Agency. (2021). *Net Zero By 2050-A Roadmap for the Global Energy Sector*. [Online]. Available: https://www.iea.org/reports/net-zero-by-2050

[2] M. Blonsky, A. Nagarajan, S. Ghosh, K. McKenna, S. Veda, and B. Kroposki, "Potential impacts of transportation and building electrification on the grid: A review of electrification projections and their effects on grid infrastructure, operation, and planning," *Current Sustainable/Renewable Energy Rep.*, vol. 6, no. 4, pp. 169–176, Dec. 2019.

[3] S. S. Ravi and M. Aziz, "Utilization of electric vehicles for vehicle-to-grid services: Progress and perspectives," *Energies*, vol. 15, no. 2, p. 589, Jan. 2022.

[4] A. Ahmadian, M. Sedghi, B. Mohammadi-Ivatloo, A. Elkamel, M. A. Golkar, and M. Fowler, "Cost-benefit analysis of V2G implementation in distribution networks considering PEVs battery degradation," *IEEE Trans. Sustain. Energy*, vol. 9, no. 2, pp. 961–970, Apr. 2018.

[5] Q. Yan, B. Zhang, and M. Kezunovic, "Optimized operational cost reduction for an EV charging station integrated with battery energy storage and PV generation," *IEEE Trans. Smart Grid*, vol. 10, no. 2, pp. 2096–2106, Mar. 2019.

[6] N. I. Nimalsiri, C. P. Mediwaththe, E. L. Ratnam, M. Shaw, D. B. Smith, and S. K. Halgamuge, "A survey of algorithms for distributed charging control of electric vehicles in smart grid," *IEEE Trans. Intell. Transp. Syst.*, vol. 21, no. 11, pp. 4497–4515, Nov. 2020.

[7] K. M. Tan, V. K. Ramachandaramurthy, and J. Y. Yong, "Integration of electric vehicles in smart grid: A review on vehicle to grid technologies and optimization techniques," *Renew. Sustain. Energy Rev.*, vol. 53, pp. 720–732, Jan. 2016.

[8] W. Vermeer, G. R. C. Mouli, and P. Bauer, "Optimal sizing and control of a PV-EV-BES charging system including primary frequency control and component degradation," *IEEE Open J. Ind. Electron. Soc.*, vol. 3, pp. 236–251, 2022.

[9] W. Vermeer, G. R. Chandra Mouli, and P. Bauer, "Real-time building smart charging system based on PV forecast and Li-ion battery degradation," *Energies*, vol. 13, no. 13, p. 3415, Jul. 2020.

[10] G. R. C. Mouli, M. Kefayati, R. Baldick, and P. Bauer, "Integrated PV charging of EV fleet based on energy prices, V2G, and offer of reserves," *IEEE Trans. Smart Grid*, vol. 10, no. 2, pp. 1313–1325, Mar. 2019.

[11] Y. He, B. Venkatesh, and L. Guan, "Optimal scheduling for charging and discharging of electric vehicles," *IEEE Trans. Smart Grid*, vol. 3, no. 3, pp. 1095–1105, Sep. 2012.

[12] C. Wu, H. Mohsenian-Rad, and J. Huang, "Vehicle-to-aggregator interaction game," *IEEE Trans. Smart Grid*, vol. 3, no. 1, pp. 434–442, Mar. 2012.

[13] M. Wang, Y. Mu, Q. Shi, H. Jia, and F. Li, "Electric vehicle aggregator modeling and control for frequency regulation considering progressive state recovery," *IEEE Trans. Smart Grid*, vol. 11, no. 5, pp. 4176–4189, Sep. 2020.
[14] S. Han, S. Han, and K. Sezaki, "Development of an optimal vehicle-to-grid aggregator for frequency regulation," *IEEE Trans. Smart Grid*, vol. 1, no. 1, pp. 65–72, Jun. 2010.
[15] J. Hu, C. Si, M. Lind, and R. Yu, "Preventing distribution grid congestion by integrating indirect control in a hierarchical electric vehicles' management system," *IEEE Trans. Transport. Electrific.*, vol. 2, no. 3, pp. 290–299, Sep. 2016.
[16] G. R. Chandra Mouli, P. Bauer, and M. Zeman, "System design for a solar powered electric vehicle charging station for workplaces," *Appl. Energy*, vol. 168, pp. 434–443, Apr. 2016.
[17] J. García-Villalobos, I. Zamora, K. Knezović, and M. Marinelli, "Multi-objective optimization control of plug-in electric vehicles in low voltage distribution networks," *Appl. Energy*, vol. 180, pp. 155–168, Oct. 2016.
[18] J. L. Cohon and D. H. Marks, "A review and evaluation of multiobjective programing techniques," *Water Resour. Res.*, vol. 11, no. 2, pp. 208–220, Apr. 1975.
[19] G. Chiandussi, M. Codegone, S. Ferrero, and F. E. Varesio, "Comparison of multi-objective optimization methodologies for engineering applications," *Comput. Math. Appl.*, vol. 63, no. 5, pp. 912–942, Mar. 2012.
[20] P. P. Singh, S. Das, F. Wen, I. Palu, A. K. Singh, and P. Thakur, "Multi-objective planning of electric vehicles charging in distribution system considering priority-based vehicle-to-grid scheduling," *Swarm Evol. Comput.*, vol. 77, Mar. 2023, Art. no. 101234.
[21] A. Kapoor, P. Gangwar, A. Sharma, and A. Mohapatra, "Multi-objective framework for optimal scheduling of electric vehicles," in *Proc. 21st Nat. Power Syst. Conf. (NPSC)*, Dec. 2020, pp. 1–6.
[22] K. Kaur, M. Singh, and N. Kumar, "Multiobjective optimization for frequency support using electric vehicles: An aggregator-based hierarchical control mechanism," *IEEE Syst. J.*, vol. 13, no. 1, pp. 771–782, Mar. 2019.
[23] H.-M. Chung, W.-T. Li, C. Yuen, C.-K. Wen, and N. Crespi, "Electric vehicle charge scheduling mechanism to maximize cost efficiency and user convenience," *IEEE Trans. Smart Grid*, vol. 10, no. 3, pp. 3020–3030, May 2019.
[24] R. Jiang, Z. Zhang, J. Li, Y. Zhang, and Q. Huang, "A coordinated charging strategy for electric vehicles based on multi-objective optimization," in *Proc. 2nd Int. Conf. Power Renew. Energy*, Sep. 2017, pp. 823–827.
[25] S. Mishra, A. Mondal, and S. Mondal, "A multi-objective optimization framework for electric vehicle charge scheduling with adaptable charging ports," *IEEE Trans. Veh. Technol.*, vol. 72, no. 5, pp. 5702–5714, May 2023.
[26] A. Kharra, R. Tiwari, J. G. Singh, and T. Rawat, "Interval optimization technique based multi-objective scheduling of electric vehicles," in *Proc. Int. Conf. Power*, 2023, pp. 1–6.
[27] J. G. Singh and R. Tiwari, "Multi-objective optimal scheduling of electric vehicles in distribution system," in *Proc. 20th Nat. Power Syst. Conf.*, 2018, pp. 1–6.
[28] S. Ruzika and M. M. Wiecek, "Approximation methods in multiobjective programming," *J. Optim. Theory Appl.*, vol. 126, no. 3, pp. 473–501, Sep. 2005.
[29] A. Zakariazadeh, S. Jadid, and P. Siano, "Multi-objective scheduling of electric vehicles in smart distribution system," *Energy Convers. Manage.*, vol. 79, pp. 43–53, Mar. 2014.
[30] Maigha and M. L. Crow, "Electric vehicle scheduling considering co-optimized customer and system objectives," *IEEE Trans. Sustain. Energy*, vol. 9, no. 1, pp. 410–419, Jan. 2018.
[31] A. H. Einaddin and A. S. Yazdankhah, "A novel approach for multi-objective optimal scheduling of large-scale EV fleets in a smart distribution grid considering realistic and stochastic modeling framework," *Int. J. Electr. Power Energy Syst.*, vol. 117, May 2020, Art. no. 105617.
[32] B. Ahmadi, N. B. Arias, G. Hoogsteen, and J. L. Hurink, "Multi-objective advanced grey wolf optimization framework for smart charging scheduling of EVs in distribution grids," in *Proc. 57th Int. Universities Power Eng. Conf., Big Data Smart Grids*, 2022, pp. 1–6.
[33] G. Mavrotas and K. Florios, "An improved version of the augmented ϵ-constraint method (AUGMECON2) for finding the exact Pareto set in multi-objective integer programming problems," *Appl. Math. Comput.*, vol. 219, no. 18, pp. 9652–9669, May 2013.
[34] G. Mavrotas, "Effective implementation of the ϵ-constraint method in multi-objective mathematical programming problems," *Appl. Math. Comput.*, vol. 213, no. 2, pp. 455–465, Jul. 2009.
[35] M. Kefayati and C. Caramanis, "Efficient energy delivery management for PHEVs," in *Proc. 1st IEEE Int. Conf. Smart Grid Commun.*, Oct. 2010, pp. 525–530.
[36] W. Vermeer, G. R. Chandra Mouli, and P. Bauer, "A comprehensive review on the characteristics and modeling of lithium-ion battery aging," *IEEE Trans. Transport. Electrific.*, vol. 8, no. 2, pp. 2205–2232, Jun. 2022.
[37] M. Lubin, O. Dowson, J. D. Garcia, J. Huchette, B. Legat, and J. P. Vielma, "JuMP 1.0: Recent improvements to a modeling language for mathematical optimization," *Math. Program. Comput.*, vol. 15, no. 3, pp. 581–589, Sep. 2023.
[38] *ENTSO-E*. Accessed: Oct. 21, 2024. [Online]. Available: https://www.entsoe.eu/
[39] *Analyses-Elaad NL*. Accessed: Oct. 21, 2024. [Online]. Available: https://platform.elaad.io/analyses.html
[40] *Elektrisch Vervoer-Personenauto's-Nederland*. Accessed: Oct. 21, 2024. [Online]. Available: https://duurzamemobiliteit.databank.nl/
[41] M. S. Alvarez-Alvarado, F. E. Alban-Chacón, E. A. Lamilla-Rubio, C. D. Rodríguez-Gallegos, and W. Velásquez, "Three novel quantum-inspired swarm optimization algorithms using different bounded potential fields," *Sci. Rep.*, vol. 11, no. 1, Jun. 2021, Art. no. 11655, doi: 10.1038/s41598-021-90847-7.

ISTVÁN BARA (Student Member, IEEE) received the bachelor's and master's degrees in mechatronics engineering from Budapest University of Technology and Economics, Hungary, in 2018 and 2021, respectively. He is currently pursuing the Ph.D. degree in electric vehicle smart charging with Delft University of Technology. His research interests include EV smart charging, multi-objective optimization, and battery degradation.

GAUTHAM RAM CHANDRA MOULI (Member, IEEE) received the bachelor's degree in electrical engineering from the National Institute of Technology Tiruchirappalli, India, in 2011, the master's degree in electrical engineering from Delft University of Technology, The Netherlands, in 2013, and the Ph.D. degree from Delft University, in 2018, for the development of a solar powered V2G electric vehicle charger compatible with CHAdeMO, CCS/COMBO, and designed smart charging algorithms (with PRE Power Developers, ABB, and UT Austin). He is currently an Associate Professor with the DC Systems, Energy Conversion and Storage Group, Department of Electrical Sustainable Energy, Delft University of Technology. His current research interests include electric vehicles, EV charging, PV systems, power electronics, and demand-side management.

PAVOL BAUER (Senior Member, IEEE) received the master's degree in electrical engineering from the Technical University of Kosice, in 1985, and the Ph.D. degree from Delft University of Technology in 1995. He is currently a Full Professor with the Department of Electrical Sustainable Energy, Delft University of Technology; and the Head of the DC Systems, Energy Conversion and Storage Group.